ISSN 0208-7774 TRIBOLOGIA 4/2018 p. 23–29

Kinga CHRONOWSKA-PRZYWARA*, Marcin KOT*, Marcin SZCZĘCH*

EFFECT OF RESIDUAL STRESS ON LOAD BEARING CAPACITY OF PVD COATED SURFACES

WPŁYW NAPRĘŻEŃ WŁASNYCH NA NOŚNOŚĆ POWIERZCHNI Z POWŁOKAMI PVD

Key words: PVD coatings, contact mechanics, residual stress, fracture toughness.

Abstract The article presents the results of spherical indentation modelling of coating-substrate systems. Modelling was carried out using the finite element method. First of all, the effect of the coating thickness on system deformation and stress distribution was taken into analysis, assuming coating thicknesses of 1, 2, and 5 μm, which are typical for tribological applications as well as models with infinitely thick coating and without a coating. The evolution of maximum radial stresses in the indentation within 0 to 3N load is presented. A significant effect of the coating thickness on the value and location of the maximum stress concentration was observed. The effect of internal stresses on surface bearing capacity with PVD coatings was also analysed. The paper presents the possibility of creating failure maps of coating–substrate systems for the assumed mechanical properties of materials, which allows one to determine the load capacity of coated surface or choose the optimal coating thickness when the maximum strength and contact geometry are known.

Słowa kluczowe: powłoki PVD, mechanika kontaktu, naprężenia własne, odporność na pękanie.

Streszczenie W artykule zostały przedstawione wyniki modelowania sferycznej indentacji układów powłoka-podłoże. Modelowanie prowadzono z użyciem metody elementów skończonych. Analizowano przede wszystkim wpływ grubości powłoki na deformacje układu i rozkład naprężeń, przyjmując typowe w tribologicznych aplikacjach grubości powłok 1, 2 i 5 μm oraz modele z nieskończenie grubą powłoką i bez powłoki. Przedstawiono ewolucję głównie przy maksymalnych naprężeniach promieniowych w zakresie obciążenia wgłębnika od 0 do 1 N. Zaobserwowano istotny wpływ grubości powłoki na wartość i miejsca maksymalnej koncentracji naprężeń. Analizowano także wpływ naprężeń własnych na nośność powierzchni z powłokami PVD. W pracy przedstawiono możliwość tworzenia map niszczenia układów powłoka–podłoże dla założonych właściwości mechanicznych materiałów, dzięki której można określić zakres nośności powierzchni układu lub dobrać optymalną grubość powłoki przy znajomości maksymalnej siły i geometrii kontaktu.

INTRODUCTION

In many friction nodes like bearings, gears, cams, and rollers, the contact between two elements take place on non-congruent surfaces. Determination of loads, deformations, and stress distributions in such elements are in the area of interests of tribologists due to their large influence on friction and wear processes. For homogeneous materials, Hertz **[L. 1–3]** was the first to give a solution for such a contact; therefore, the term "Hertz contact" is usually used, and equations are called Hertz's formulas. However, they are valid only for the contact of elements with homogeneous properties. However, it cannot be used for elements on which the technological surface layers were created or coatings with other properties than the core material were deposited; however, technologies of surface strengthening are presently commonly used. The main reason the Hertz's theory cannot be applied in such cases is the mismatch of the elastic properties of the coating/surface layer and substrate. Furthermore, surfaces after modification are often subjected to residual stresses. PVD coatings can undergo stresses, usually compressive, at the level of several GPa **[L. 4]**. Hertz's theory is limited only to elastic deformation and does not allow one to take into account the local plastic deformation that can occur in

* AGH University of Science and Technology, Faculty of Mechanical Engineering and Robotics, 30-065 Kraków, al. Mickiewicza 30, Poland, e-mail: chronows@agh.edu.pl.

the substrate with lower hardness below the coating. Moreover, it is not possible to calculate tensile stress on the surface that lead to crack formation just outside the contact zone, which is usually observed for brittle ceramic and carbon coatings. There are other formulas in publications that take into account different properties of coating and substrates **[L. 5]** and the existence of tangential forces due to friction. However, there are not many studies in which the residual stress in coating-substrate systems and the local plastic deformation of the substrates were taken into account.

An effective tool that enables analysis of contact mechanics of coated surfaces is the finite element method (FEM). Many papers have appeared recently in which the contact of coated elements were modelled, and the most commonly analysed model is flat surface with a coating with a spherical indenter pressed into it **[L. 6–10]**. This is due to the fact that such a contact is common in machines, and there is an experimental verification for real elements of such geometry by new research techniques, e.g., indentation with continuous measurement of force and penetration depth or scratch tests. In both of these tests, spherical indenters can be used, which gives one the opportunity to direct the comparison of the experimental with modelling results. The effects of such combined analyses are proposed by the authors' failure maps of coated systems defined in t/R_i (coating thickness/indenter radius) vs. F/R_i^2 (destructive force/indenter radius) coordinates. This allows one to eliminate the indenter geometry and coating thickness and to predict critical loads for any contact geometry **[L. 6, 11]**. The paper **[L. 12]** presents analyses using various indenters, giving different ratios of the indenter radius to coating thickness, which results in a different character of stress distribution in coated systems. The determination of permissible loads enables avoiding catastrophic forms of wear caused by excessive deformation and yield of the substrate. These deformations with applied hard, brittle coatings that lead to the fracture and destruction of the tribological system and significant wear intensification **[L. 13, 14]**. In the case of coatings, the tensile stress is the most commonly accepted strength criterion that predicts the destruction. Besides the stresses as result of external loading, the residual stresses from the coating's deposition process also exists.

This raises the question whether the allowable stresses leading to crack formation in a coating could be calculated by subtracting residual stress from applied stress resulting from external load and hence adopting the fracture criterion as follows:

$$\sigma_{app} - \sigma_{res} \leq \sigma_{fr}$$

where σ_{app} – applied stress, σ_{res} – residual stress, σ_{fr} – critical stress causes coating fracture.

RESEARCH METHODS

Analytical model

Hertz's theory allows one to calculate contact stresses at a known geometry and mechanical properties of both materials. However, it cannot be used when the material properties change, i.e. for gradient materials, or coated surfaces. Therefore, the FEM analysis was applied for analyses that were subsequently carried out for coating-substrate systems. For comparison with analytical relationships, FEM experiments were also done for two threshold cases: the uncoated substrate and the substrate with a coating thick enough that the deformation did not reach substrate, thus the model could substitute a homogeneous material with coating's properties. Using Hertz's relations, it is possible to calculate the contact stress distribution in the contact zone as well as just outside it.

In the paper the equations (1-8) for sphere-plane contact were used **[L. 15–21]**. The mean pressure p_m in the contact area and contact radius a_c were calculated from the following equations (1) and (2), respectively:

$$p_m = \frac{F}{\pi \cdot a_c^{\,2}} \tag{1}$$

$$a_c = \sqrt[3]{\frac{3 \cdot F \cdot R}{4 \cdot E_{zred}}} \tag{2}$$

where F – normal force, R – sphere radius, a E_{zred} – reduced elasticity modulus calculated as follows:

$$E_{zred} = \frac{1}{\dfrac{1-\vartheta_1^2}{E_1} + \dfrac{1-\vartheta_2^2}{E_2}} \tag{3}$$

where E_1, E_2, ϑ_1, ϑ_2 – Young's modulus and Poisson ratio of ball and flat sample materials.

Whereas, the maximal contact stress in the central point of contact zone p_O reaches the following value:

$$p_o = \frac{3}{2} \cdot p_m \tag{4}$$

The radial and circumferential stress distributions within contact zone $r \in (0; a_c)$ were found from Equations (5) and (6):

$$\sigma_{rr}(r) = p_o \frac{1-2\cdot\vartheta_2}{3}\left(\frac{a_c^2}{r^2}\right)\cdot\left[1-\left(1-\frac{r^2}{a_c^2}\right)^{\frac{3}{2}}-\left(1-\frac{r^2}{a_c^2}\right)^{\frac{1}{2}}\right] \tag{5}$$

$$\sigma_{\theta\theta}(r) = p_o \frac{1-2\cdot\vartheta_2}{3}\left(\frac{a_c^2}{r^2}\right)\cdot\left[\left[1-\left(1-\frac{r^2}{a_c^2}\right)^{\frac{3}{2}}-2\cdot\vartheta_2\left(1-\frac{r^2}{a_c^2}\right)^{\frac{1}{2}}\right]\right. \tag{6}$$

The normal stress distribution along the z-axis, i.e. along the model symmetry axis was also analysed as follows:

$$\sigma_{zz}(r) = p_o\left[-1\left(1-\frac{r^2}{a_c^2}\right)^{\frac{1}{2}}\right] \quad (7)$$

For brittle materials, for which tensile stresses are taken as the main failure criterion, the most important are radial stresses outside the contact zone, which for $r \in (a_c; 1,5a_c)$ r can be determined from the following:

$$\sigma_{rr}(r) = -p_o\left[\frac{(1-2\cdot\vartheta_2)\cdot a_c^2}{3\cdot r^2}\right] \quad (8)$$

Unfortunately, Hertz's theory does not allow one to determine the stress distribution along coating–substrate interface, while the authors' previous studies indicate that this could be area of coating crack formation **[L. 6, 11, 14]**. From Equations (1–8), stress distributions for homogeneous materials, an uncoated substrate and infinitely thick coating, were calculated. The same material parameters of coating and substrate, summarized in the **Table 1**, were adopted in the analytical model and finite element method.

FEM modelling

The numerical analysis using the finite element method (FEM) was carried out using Ansys software on a high-power computer in ACK CYFRONET UST-AGH. Coating-substrate systems were modelled as well as infinitely thick coatings and uncoated substrates. A diamond indenter with a ball geometry and R = 20 μm radius was pressed into models, using a normal force within the range 0-1 or 0-3 N (which depends on coating thickness) with a 0.1 N constant load increase in subsequent steps. The coating thicknesses were 1, 2, and 5mm, which corresponds to the most frequently used range of PVD coatings for mechanical application. The axisymmetric model was adopted for numerical calculations, which allowed reducing calculation time. Finite elements in the models were Plane182 quadrangles with 4 nodes placed in the corners. The nodes in the symmetry axis cannot deform along the X-Y plane, and the finite element grid was denser in the vicinity of indentation region. For coating–indenter contact, slip was permitted with an assumed coefficient of friction μ = 0.1, determined from the scratch tests performed and applied in the modelling load range. For the substrate, a Bilinear Isotropic Hardening model of material properties with possible yielding but with no strengthening during plastic flow was defined, while the coating and indenter are assumed to be perfectly elastic. FEM calculations were also done for these models with additionally added residual stresses. Stresses were introduced by deformation due to temperature changes and the difference in thermal expansion of coating and substrate. In order to shorten the calculation time, due to axial symmetry of models, the 3D model was simplified to a 2D flat one and half of this was considered, which was possible after assuming the appropriate boundary conditions given above.

Analysed materials

The material parameters of coating, substrate, and diamond adopted for analysis are listed in **Table 1**. Two values of internal stresses 2 and 5 GPa in the coating, both compressive and tensile, were assumed and compared with models without residual stress.

Table 1. Materials parameters adopted in modelling
Tabela 1. Parametry materiałowe powłoki i podłoża użyte do modelowania

Element of model	Young's modulus E [GPa]	Yield strength R_e [MPa]	Poisson ration ϑ
Substrate	210	800	0.3
Coating	420	-	0.25
Diamond ball	1041	-	0.07

The total stress occurring in the coating-substrate systems is a superposition of stress originating from external loads and contact with the tribological partner or roughness peaks and residual stress, which, after many vacuum deposition processes, may reach several GPa. In literature, the effect of this stress has been presented in only a few studies so far, and there is no systematic work on this field. Therefore, the next step in analysis carried out was the introduction of residual stress and an analysis of how it affects the mechanical response of coated surface. The values of this compressive stress, measured mainly by the XRD method, are typical for ceramic coatings. Tensile stresses were also found (of course not as high as 5 GPa) in the case of electroplated coatings. The aim of the analysis is to check if, under high contact stress and local plastic deformation of substrate, residual stress could be simply added with stresses originating from external loads. This is an important issue for the designer, who knowing the residual stresses in the coating, e.g., from X-ray examinations, could enter them into calculations and check whether, after applying higher external loads, the system is still on the safe side that provides no crack formation in the coating.

EXPERIMENTAL RESULTS

For coatings deposited on softer substrates, the main mechanism of surface failure is the coating fracture. Such cracks are related to the coatings bending below indenter and outside the contact zone. The most frequently observed circular cracks after

spherical indentation arise as a result of radial stress concentrations on coating surface. **Figure 1** compares the distribution of radial stresses under 0.2 N load in modelled systems. Arrows denote the contact radii a_c for systems with 1, 2, and 5 μm coating thicknesses. A large difference in the contact radius was observed for uncoated substrate in the analytical and FEM models. The Hertz model works within the elastic state of deformation, while substrate yield, even at this low load, was observed in FEM results. This plastic deformation reduces mean contact pressure in the contact zone by the rise of contact area. Moreover, this stress cannot exceed the material›s hardness. Whereas, the contact radius for the substrate is much larger in relation to infinitely thick coating, and then the mean stress for the second model is significantly larger, and strengthened by a 200% higher elasticity modulus compared to the substrate. The results for the thickest coating of 5 μm are similar to the results for the infinitely thick coating, which indicates that the substrate does not have a significant impact on the deformation of the entire system. In addition, the change of radial stress values from compressive to tensile appears at a higher distance from contact zone for thinner coatings. It is the result of substrate plastic deformation and weaker coating bending outside the contact area with indenter.

With rise in normal load, the maximum stress outside the contact zone rises, which could lead to brittle fracture. The evolution of the maximum stress with increasing load for the analysed models is shown in **Figure 2.** At the tested load range for the 5 μm thick

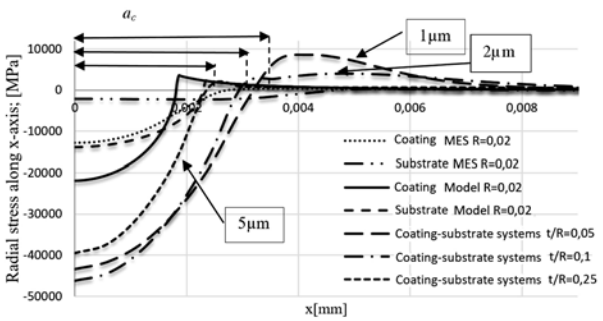

Fig. 1. Radial stresses on coating surface for systems with t = 1, 2, and 5 μm coating thickness, models with infinitely thick coating (MES coating R = 0.02), infinitely thick substrate (substrate MES R = 0.02) and for analytical models with an infinitely thick coating (Coating Model R = 0.02) and infinitely thick substrate (Substrate Model R = 0.02) with 20 μm sphere radius at 0.2 N load.

Rys. 1. Naprężenia promieniowe na powierzchni powłoki dla układów z powłoką t = 1, 2 i 5 μm, modeli z nieskończenie grubą powłoką (Powłoka MES R = 0,02) i nieskończenie grubym podłożem (Podłoże MES R = 0,02) oraz dla modeli analitycznych z nieskończenie grubą powłoką (Powłoka Model R = 0,02) i nieskończenie grubym podłożem (Podłoże Model R = 0,02) dla promienia kuli 20 μm i siły 0,2 [N]

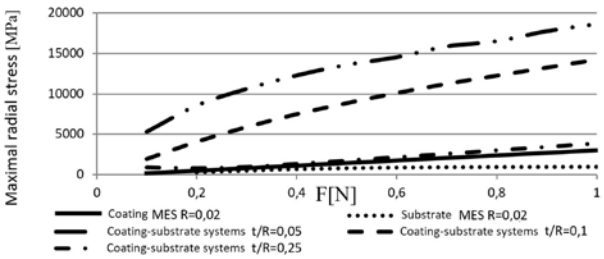

Fig. 2. Maximum radial stresses on coatings surface as a function of external load on spherical indenter with 20 μm radius

Rys. 2 . Maksymalne naprężenia promieniowe na powierzchni powłoki w funkcji siły obciążającej wgłębnik o promieniu 20 μm

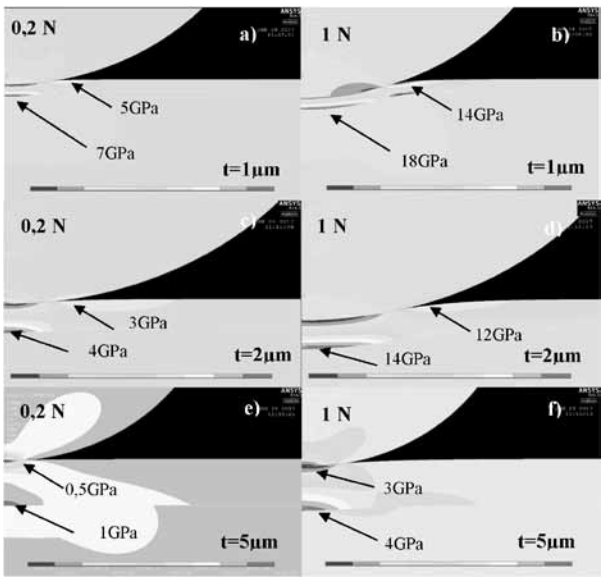

Fig. 3. Radial stresses distribution for: a) 1 μm coating at 0.2 N load, b) 1 μm coating at 1 N load, c) 2 μm coating at 0.2 N load, d) 2 μm coating at 1 N load, e) 5 μm coating at 0.2 N load, f) 5 μm coating at 1 N load

Rys. 3. Rozkład naprężeń promieniowych dla powłok 1, 2, 5 przy sile 0,2 [N] i 1 [N]: a) układ z powłoką 1 μm przy sile 0,2 [N], b) układ z powłoką 1 μm przy sile 1 [N], c) układ z powłoką 2 μm przy sile 0,2 [N], d) układ z powłoką 2 μm przy sile 1 [N], e) układ z powłoką 5 μm przy sile 0,2 [N], f) układ z powłoką 5 μm przy sile 1 [N]

coating (t/R = 0.25), as indicated before, the maximum radial stress is close to its value for the model with the infinitely thick coating. FEM analysis showed that load 1N induced radial stress equal to 4 GPa, while thinner coatings do not restrict the system deformation, and maximum radial stress grows rapidly reaching 18 and 14 GPa at 1 N for 1 and 2 μm coatings, respectively. These levels of tensile stress on surface must lead to brittle fracture of typical tribological coatings. Distributions of radial stresses derived from FEM calculations are shown in **Figure 3**. For 1 and 2 μm coatings (**Figures 3a–d**), a high concentration of radial stresses 5 and 7 GPa

(at 0.2 N load) are visible on coating-substrate interface on the indenter axis and on the surface of the coating just outside the contact zone, respectively. Moreover, at 1N load, they reach 14 and 18GPa (**Figure 3b**). For the thickest coating, the maximum stresses occur at the interface, and stresses at surface are much smaller (**Figs. 3e–f**). However, compressive residual stresses can significantly onset coatings fracture. Values of maximum radial stresses, for 0.2 N and 1N loads for 1 and 5 μm coatings, with taking into account the introduced residual stresses, are shown in **Figure 4**. The maximum tensile stresses 23 GPa at 1N load for the 1 μm coating reduces to 15GPa when the residual, compressive stress is 5GPa (**Fig. 4a**). Similarly, for the 5mm coating, one can notice the stress drop from 4 to -1 GPa. However, after residual stress subtraction for all models with the same coating thickness, the stress distributions are similar (**Fig. 4b**). Small differences were found for the thinner coating, where the remaining stresses were lower in a case of initial compressive residual stresses than for tensile stresses. This is probably the result of a smaller plastically deformed zone in the substrate and consequently lower coating bending. However, the difference is 1GPa in relation to the model without residual stress.

The evolution of maximal radial stresses as a function of increasing system deformations defined as h/t – relative penetration depth (h – penetration depth / t – coating thickness) with an increasing load to 1 N and 3 N for 1 and 5 μm coatings are shown in **Figure 5**. For both coatings, the rise of penetration depth caused an increase of maximum radial stress. The lower value of compressive residual stresses, the greater is the value of the maximum radial stresses at the same depth of penetration. The compressive residual stress reduces maximum total radial stresses on the coating's surface. For 5GPa compressive stresses and the thinnest coating, the maximum radial stress was reduced from 19 GPa to 14 GPa, while, for the thickest coating, from 4.5 GPa to -0.5GPa. These stress reductions within the whole deformation range are very similar and close to residual stresses values.

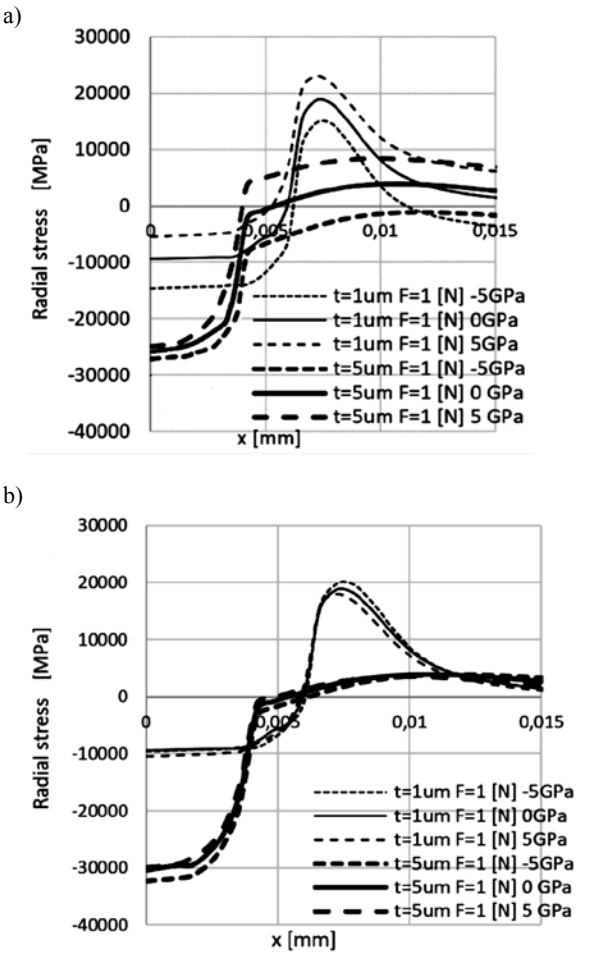

Fig. 4. Radial stress along coating surface at 1 N load: a) with residual stress, b) after subtracting residual stress

Rys. 4. Maksymalne naprężenia z uwzględnieniem naprężeń własnych na styku kula-powierzchnia dla siły 1 N: a) z uwzględnieniem naprężeń własnych, b) po odjęciu naprężeń własnych

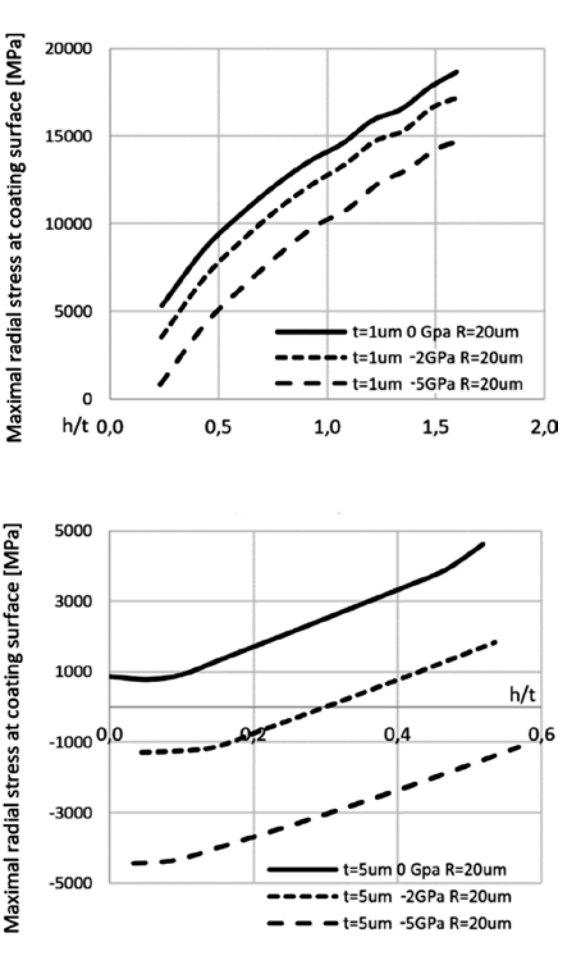

Fig. 5. Maximum radial stresses vs. relative penetration depth h/t for: a) 1 μm coating at F = 1 N load, b) 5 μm coating at F = 3 N load

Rys. 5. Maksymalne naprężenia promieniowe w funkcji h/t a) siły F = 1 [N] dla powłoki 1μm b) siły 3 [N] dla powłoki 5 μm

Assuming the critical stresses causing coating fracture at the level of 5 GPa, a failure map of the coating-substrate system was created and shown in **Figure 6**. To break free from contact geometry and real loads, these values were divided by indenter radius and the square of the indenter radius, respectively, which gave a t/R and F/R^2 coordinate system. It is clearly seen that the increase of F/R^2 is not linear as a function of the relative coating thickness t/R. However, the increase of compressive residual stresses from -2 to -5 GPa enhanced the load bearing capacity of the analysed systems by 50%. However, one must be careful with the conclusion that thicker coating are better, because as the thickness of the PVD coating increases their adhesion to the substrate, but it then usually decreases due to higher stress concentration at coating-substrate interface derived from the typical mismatch of elasticity modulus of both materials.

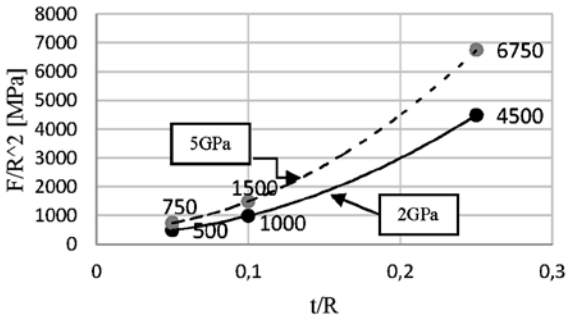

Fig. 6. Failure map of coating–substrate system (for coatings with t = 1, 2.5µm thickness, R = 20 µm indenter radius and compressive residual stress 2 and 5 GPa)

Rys. 6. Mapa deformacji układu powłoka–podłoże (dla powłok o grubości odpowiednio T = 1, 2, 5 µm, R wgłębnika 20 µm i wprowadzonych naprężeniach własnych 2 i 5 GPa)

CONCLUSIONS

The results of spherical indentation modelling of coating-substrate systems allowed assessing the effect of the coating thickness on deformation and stress distribution for a typical thickness of tribological coatings deposited by PVD methods. Analysing the maximum radial stresses, it was noticed that, for the 5 µm thick coating (relative penetration depth t/R = 0.25), the substrate has a negligible effect and the results are comparable to the model with infinitely thick coating. However, thinner coatings with t/R = 0.05-0.1 do not restrict extensive system deformation due to easy substrate yield. At a 1N load, this deformation cause extremely high radial stresses that have to lead to coatings fracture, while they may be much smaller when the compressive residual stresses exist in the coating after deposition process. The same analysed models with and without residual stress allowed us to answer the main question in this work of whether the residual stress and stress originating from external loads could be added, even despite the occurrence of plastic deformations of the substrate. The analysis of the maximum radial stresses for coatings of all coating thickness, with residual stress ranging from -5 to +5 GPa, proved that, after subtracting them for all models with the same coating thickness, the stress distributions from external loads are similar. A slight difference of 1GPa in radial stress for the thinnest coating (t = 1 µm) was observed, which was probably caused by well-developed substrate yield and thus a smaller bending of the coating. Additionally, the proposed failure map of analysed coating-substrate systems could be a helpful tool for designing coated systems. It predicts permissible loads in a selected friction node with known residual stresses, e.g., 5 GPa. The effect of residual stress could be very strong, which was confirmed by an increase of 50% of load bearing capacity of the analysed systems with the rise of residual compressive stresses from -2 to -5 GPa.

ACKNOWLEDGEMENT:

This work is financed by AGH University of Science and Technology, Faculty of Mechanical Engineering and Robotics, research program no. 15.11.130.834

REFERENCES

1. Hertz H.: Verhandlungen des vereins zur Beforderung des Gewerbefleisses,, Novenber, Leipzig, 1982, 163–183.
2. Tabor D.: Hardness of Metals, Clarendon Press, Oxford (1951).
3. Johnson K.L.: Contact Mechanics, Cambridge University Press, Cambridge 1985.
4. Akonoa A.T., Ulmb F.A: An improved technique for characterizing the fracture toughness via scratch test experiments,Wear, 313, 2014.
5. Esqué-de los Ojosa, James D., Besta P., Schwiedrzik A., Morsteinb M., Michlera J: A closed-form analytical approach for the simple prediction of hard-coating failure for tooling systems, Surface & Coatings Technology|, 2016.

6. Michler J., Blank U.E.: Analysis of coating fracture and substrate plasticity induced by spherical indentors: diamond and diamond-like carbon layers on steel substrates, Thin Solid Films 381 2001 119–134.
7. Zhang G.A.,, Wu Z.G., Wang M.X., Fan X.Y., Wang J., Yan P.X.: Structure evolution and mechanical properties enhancement of Al/AlN multilayer. Applied Surface Science, 253 (2007) 8835–8840.
8. Souza R.M., Sinatora A., Mustoe G.G.W., Moore J.J.: Numerical and experimental study of the circular cracks observed at the contact edges of the indentations of coated systems with soft substrates. Wear 251 (2001) 1337––1346.
9. Pe´rez E.A., Souza R.M.: Numerical and experimental analyses on the contact stresses developed during single and successive indentations of coated systems. Surface and Coatings Technology 188–189 (2004) 572–580.
10. Pachler T., Souza R.M., Tschiptschin A.P.: Finite element analysis of peak stresses developed during indentation of ceramic coated steels. Surface and Coatings Technology 202 (2007) 1098–1102.
11. Kot M., Rakowski W., Major Ł., Lackner J.: Load-bearing capacity of coating-substrate systems obtained from spherical indentation tests. Materials and Design, 46, 2013.
12. Kot M.: Analiza właściwości mechanicznych układów powłoka–podłoże przy użyciu metody indentacji z wykorzystaniem wgłębników o różnej geometrii. Tribologia, vol. 236 (2011) 47–60.
13. Kot M., Rakowski W., Morgiel J., Major Ł.: Metoda wyznaczania nacisku dopuszczalnego w styku skoncentrowanym dla układów powłoka–podłoże. Tribologia, vol. 218 (2/2008), pp. 285–295.
14. Kot M., Rakowski W., Lackner J.M., Major Ł.: Analysis of spherical indentations of coating-substrate systems: Experiments and finite element modeling. Materials and Design 43 (2013) 99–111.
15. Niezgodziński M., Niezgodziński T., Wzory, wykresy i tablice wytrzymałościowe, PWN, Warszawa 1977.
16. Anthony C., Fischer-Cripps, Nanoindentation, Mechanical Engineering Series, Springer, 2001.
17. Williams J.A., Dwyer-Joyce R.S.: Modern Tribology Handbook- Contact between solid surfaces, CRC Press LLC, 2001.
18. Wang T., Wang L., Zheng L.G.: Stress analysis of elastic coated solids in point contact, Tribology International 86, 2015, p. 52-61.
19. Steve G., Charles W., Yordanos B., Determination of residual stress in brittle materials by Hertzian indentation: Teory and experiment, Journal of the American Ceramic Society, 1999, vol. 82.
20. Tang K.C., Faulkner A., Schwarzer N., Arnell R.D., Richter F.: Comparison between an elastic-perfectly plastic finite element model and a purely elastic analytical model for a spherical indenter on a layered substrate, Elsevier. Thin Solid Films, 1997, p. 177–188.
21. Muchler J., Blank E.: Analysys of coating fracture and substrate plasticity induced by spherical indentors: diamond and diamond- like- carbon layers on steel substrates, Elsevier. Thin solid Films, 2001, p. 119–134.